Structure, Vol. 9, 177–184, February, 2001, ©2001 Elsevier Science Ltd. All rights reserved. PII S0969-2126(01)00570-6

Crystal Structures of the HslVU Peptidase–ATPase Complex Reveal an ATP-Dependent Proteolysis Mechanism

J. Wang,*§ J. J. Song,† M. C. Franklin,* S. Kamtekar,* Y. J. Im,† S. H. Rho,† I. S. Seong,‡ C. S. Lee,‡ C. H. Chung,‡ and S. H. Eom†§

*Department of Molecular Biophysics and Biochemistry
266 Whitney Avenue
Yale University
New Haven, Connecticut 06520

†Department of Life Science
Kwangju Institute of Science and Technology (K-JIST)
Kwangju 500-712
Korea

‡School of Biological Sciences
Seoul National University
Seoul 151-742
Korea

Summary

Background: The bacterial *h*eat *s*hock *l*ocus HslU ATPase and HslV peptidase together form an ATP-dependent HslVU protease. Bacterial HslVU is a homolog of the eukaryotic 26S proteasome. Crystallographic studies of HslVU should provide an understanding of ATP-dependent protein unfolding, translocation, and proteolysis by this and other ATP-dependent proteases.

Results: We present a 3.0 Å resolution crystal structure of HslVU with an HslU hexamer bound at one end of an HslV dodecamer. The structure shows that the central pores of the ATPase and peptidase are next to each other and aligned. The central pore of HslU consists of a GYVG motif, which is conserved among protease-associated ATPases. The binding of one HslU hexamer to one end of an HslV dodecamer in the 3.0 Å resolution structure opens both HslV central pores and induces asymmetric changes in HslV.

Conclusions: Analysis of nucleotide binding induced conformational changes in the current and previous HslU structures suggests a protein unfolding–coupled translocation mechanism. In this mechanism, unfolded polypeptides are threaded through the aligned pores of the ATPase and peptidase and translocated into the peptidase central chamber.

Introduction

ATP-dependent proteases are responsible for the degradation of the majority of proteins in the cell [1–3], including regulatory protein factors and abnormally folded proteins. They are essential for cellular maintenance and their biochemical properties have been studied extensively over the past decade [3–5].

§To whom correspondence should be addressed (e-mail: wang@mail.csb.yale.edu [J. W.]; eom@kjist.ac.kr [S. H. E.]).

The bacterial ATP-dependent protease HslVU is a homolog of the eukaryotic 26S proteasome [6–10]. HslVU is composed of two distinct polypeptides, the *h*eat *s*hock *l*ocus HslV peptidase and HslU ATPase. HslV forms a dodecamer of two back-to-back stacked hexameric rings. HslU forms a hexameric ring and binds to either one or both HslV ends.

Crystallographic studies of the proteolytic cores of ATP-dependent proteases [11–15] reveal that they have a common architecture and underlying ATP-dependent proteolysis mechanism. One element of this common architecture is a large proteolytic chamber formed by the peptidases in two stacked rings. The proteolytic active sites are located inside this chamber and access to the chamber is restricted to narrow pores at each end. The dimensions of these pores are so small that folded proteins cannot pass through, requiring protein substrates to be in an unfolded, extended conformation in order to reach the proteolytic active sites. Electron microscopic (EM) image reconstruction [16–18] reveals that the ATPase particles in ClpAP and the 26S proteasome also have pores and the pores of the ATPases and peptidases appear to be adjacent to each other and aligned.

We have determined the crystal structures of the HslVU peptidase–ATPase complex in an asymmetric and symmetric form. The quaternary arrangement of the peptidase and ATPase in our structures is radically different from that determined previously by X-ray crystallography [19], but is consistent with the EM images of the HslVU complex [18]. Our structures also differ from the previous crystal structure [19] in the conformation of the bound nucleotide. The biological relevance of these structures is addressed below.

Results and Discussion

Structure Determination and Overall Structure

We have determined two crystal structures (Figure 1) of the HslVU protease, an asymmetric complex at 3.0 Å resolution and a symmetric complex at 7.0 Å resolution (Table 1). X-ray diffraction data in both crystal forms suffered from complete (50%:50%) hemihedral twinning. In the asymmetric complex, there is one HslU hexamer bound to end of the HslV dodecamer in a $U_6V_6V_6$ configuration (Figure 1b). In the symmetric complex, there are two HslU hexamers bound to both HslV ends in a $U_6V_6V_6U_6$ configuration (Figure 1c). Consistent with this, the length of the unit cell's *c* axis in the high-resolution crystal form (Form I; Table 1) can accommodate only one asymmetric complex, and it can accommodate one symmetric complex in the low-resolution crystal form (Form II; Table 1). The structures were determined, by molecular replacement, with the hexameric HslU and dodecameric HslV of Bochtler et al. [19] as search models. The asymmetric model has a free R factor of 29.5%

Key words: HslVU; ATP-dependent proteolysis; protein unfolding; translocation

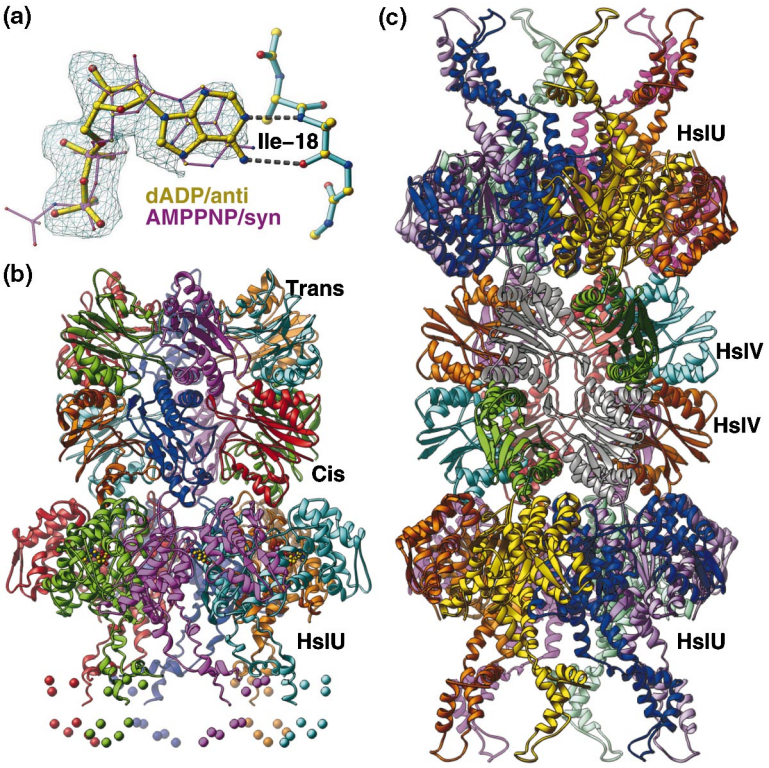

Figure 1. The Structures of HslVU

(a) A composite-omit electron density map (cyan, contoured at 1σ) at 3.0 Å resolution reveals that the bound dADP (yellow) is in an *anti* conformation, not *syn*, as in a previously determined structure (AMPPNP, magenta). This map was generated before dADP was built into the model.

(b) The HslVU complex in the asymmetric $U_6V_6V_6$ configuration. Parts of HslU domain I could not be built into the final electron density and are indicated by spheres for their approximate locations.

(c) The HslVU structure in the symmetric $U_6V_6V_6U_6$ configuration. The orientation of the complexes in (1b) and (1c) differs by 30°.

for data between 85 and 3.0 Å (Table 1). A portion of an unbiased composite-omit electron density map is shown in Figure 1a. This map was calculated before dADP was built into the structure. The symmetric model was refined with one body per subunit in the rigid-body refinement. This model has a free R factor of 43.2% for data between 10 and 7 Å (Table 1). There is a relative rotation of 6.5° of the hexameric HslU with respect to the dodecameric HslV between these two structures.

Quaternary Arrangement of the ATPase and Peptidase in the HslVU Structures

HslU can be divided into three domains [19]—amino terminal (N; residues 2–109/244–332), intermediate (I; residues 110–243), and carboxyl terminal (C; residues 333–443). In the structure of Bochtler et al., [19], HslV is contacted by HslU through domain I and the pores of HslU and HslV are separated more than 80 Å, whereas in ours this contact is mediated by the nucleotide binding domains, and the pores of HslU and HslV are next to each other and aligned. Two lines of evidence indicated that our structures are biologically more relevant. First, our structures agree with an EM structure, which shows most of the HslU's scattering mass is adjacent to HslV, with less massive domains extending away from the interface [18]. The dimension and positions of the bulky domains correspond to those of our N and C domains, and the domains with less scattering mass correspond to domain I in our structures. Second, a sequence comparison indicates that the HslU–HslV interface we observe is composed of conserved residues, as would be expected for a functionally critical interface (Figures 2a and 3a). Conserved residues are clustered into two groups on the surface, one near the pore including GYVG of the pore 1 motif and D271 at the end of the pore 2 motif (Figure 2a), and the other near the nucleotide binding site including the P loop and residues near A309 (Figure 3a). The end of HslU domain I, where HslV binds in the structure previously determined [19], is not conserved (Figure 2a). Further crystallographic resolution of differing quaternary arrangements of the peptidase and ATPases will be addressed elsewhere.

Binding of HslU to HslV Opens the HslV Translocation Pores

The binding of HslU to one HslV end induces associated asymmetric changes (Figures 3b and 3c) in electrostatic potential, surface curvature, pore size, and the peptidase active site. We define the hexameric ring of HslV as *cis* and *trans* with respect to HslU (Figure 1b). The rms Cα deviation of uncomplexed HslV [13] to *cis* HslV is 1.6 Å, and it is 2.0 Å to *trans* HslV. The *cis* and *trans* rings themselves differ by 2.3 Å. Other differences include subtle changes around the peptidase active sites, including a repositioning of K33 and a rotation of a peptide bond near Thr-1 in the *trans* ring.

Some of the most interesting changes upon the binding of HslU to HslV involve HslV's central (or translocation) pore (Figures 3b and 3c). In the uncomplexed HslV structure [13], the diameter of its translocation pore is about 13 Å, while in our $U_6V_6V_6$ structure, the *cis* HslV ring has a pore diameter of 19.7 Å, and the *trans* HslV ring has a pore diameter of 17 Å (Figures 3b and 3c). One possible advantage of opening the *trans* HslV pore

Table 1. Summary of Crystallographic Data

Form	I	II
Space group	P321	P321
Unit cell dimension	a = b = 167.00 Å, c = 161.32 Å α = β = 90°, γ = 120°	a = b = 173.39 Å, c = 254.43 Å α = β = 90°, γ = 120°
Resolution	85–3.0 Å	80–7.0 Å
R_{symm}	13.1%	20.1%
# Reflections	46,551	6,489
Completeness	86%	87%
Model content	2dADP, 4HslV 1–173 2HslU 2–131/220–443	4HslV 1–173 4HslU 2–166/216–443
Missing residues	11%	8%
rms bond length deviations	0.009 Å	(rigid-body refined)
rms bond angle deviations	1.6°	
R-factor	25.7% (85–3.0 Å)	40.1% (10–7 Å)
Free R-factor	29.5% (85–3.0 Å)	43.2% (10–7 Å)
X-ray data/PDB accession	1G4A	1G4B

$R_{symm} = \Sigma_{isym,hkl}|I - \langle I\rangle|/\Sigma_{isym,hkl}\langle I\rangle$, where *isym* are symmetry-related observations. Test set for free R-factor calculations was selected in 10% reflections in P622, taking account of twinning.

is that it might facilitate the release of proteolytic oligopeptide products through this pore.

The structure does not directly show how conformational changes in the *trans* HslV ring are transmitted through the HslV–HslV interface. It is interesting to note that the HslV–HslV interface is largely hydrophobic, and 70% of the buried 12,630 Å^2 solvent accessible area [20] at the interface involves carbon atoms. In contrast, the HslU–HslV interface is largely hydrophilic, and 50% of the buried 5,580 Å^2 solvent accessible area at the interface involves oxygen and nitrogen atoms. The buried HslU surface is conserved (Figure 3a) and includes 36 hydrogen bonds between the ATPase and peptidase.

Sequence Conservation in Domain I and Translocation Pore

Conserved HslU sequences are also exposed in two additional areas: in domain I and in the central pore of the HslU hexamer (Figure 2a). Bochtler et al. [19] have previously proposed that domain I binds unfolded protein substrates on the basis of its conformational flexibility in different crystal forms. By mapping the sequence conservation in this region onto the current structures (Figure 2a), we observe that the domain I surface facing the central cavity is conserved. This provides further evidence for their proposal that domain I is a substrate binding site. As an extension to this proposal, we believe

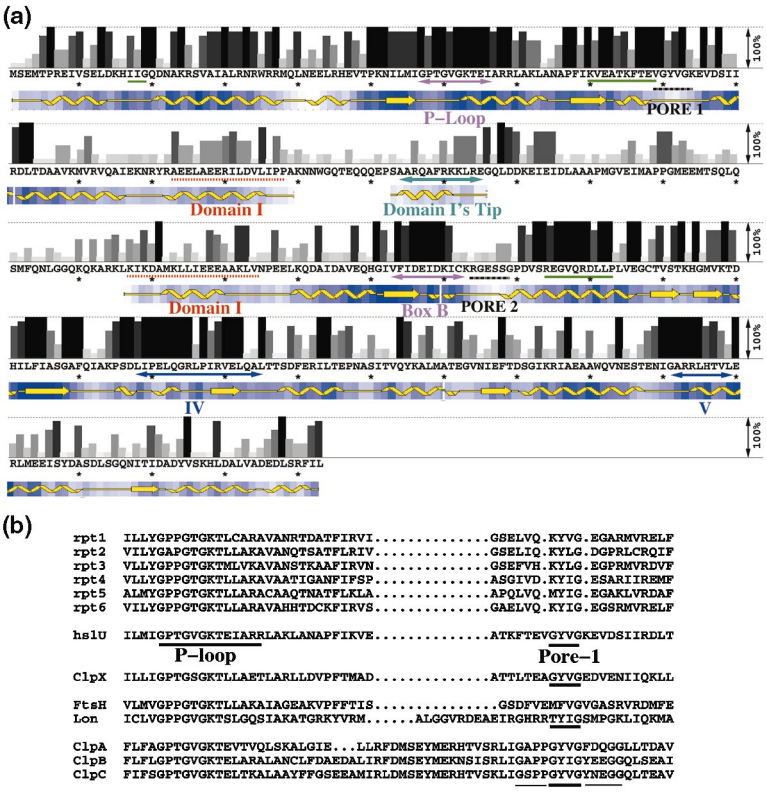

Figure 2. Sequence Conservation in HslU and Other ATPases

(a) HslU sequence conservation is shown in gray scale from the most (dark) to least (white) conserved and is compared with solvent accessibility of each residue shown in scale from buried (dark blue) to exposed (light blue and white). The secondary structures (yellow ribbons drawing), and key segments such as P loop, pore 1, pore 2, domain I, and box B (switch I) are also shown. Each 10th HslU residue is labeled with an asterisk. Walker box A (or P loop) and box B are underlined with magenta arrows. Residues at the nucleotide binding pocket are underlined in green. Motifs IV and V of the Hsp100/ClpP ATPases are underlined with blue arrows. These motifs are located at the junction of domains N and C and control the domain motion upon nucleotide binding. The ordered portion of domain I is underlined with red dashes, and the ends of the domain are underlined with green arrows. Residues in primary and secondary pores (pore 1 and pore 2) are underlined with black dashes.

(b) The conservation of the primary pore 1 motif includes all subfamilies of ATP-dependent proteases and ClpB and Hsp104. ClpA, ClpX, ClpC, ClpB, Hsp104, HslU, Lon, and FtsH are from *E. coli*, ClpC from *Synechococcus sp. PCC 7942*, and *rpt* from yeast.

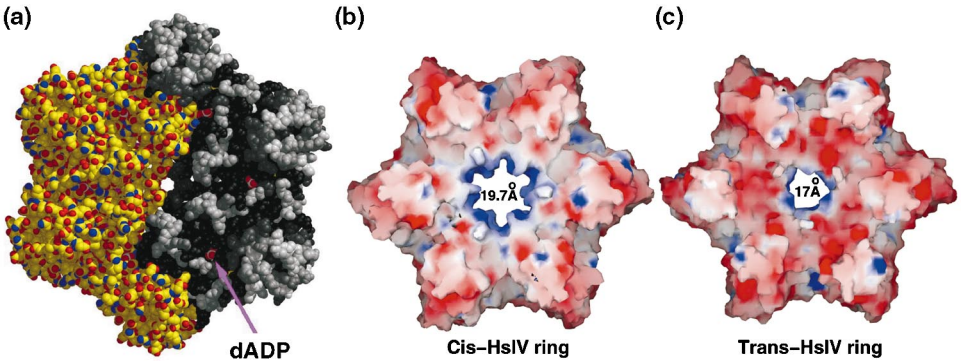

Figure 3. HslVU Complex Formation

(a) The HslU apical surface that binds HslV is hydrophilic (left side, red and blue for O and N atoms) and conserved (right side, using the same gray scale as in Figure 2). The bound dADP has a widened pore and is also shown near the apical surface.

(b) The *cis* HslV apical surface that binds HslU is also hydrophilic.

(c) The *trans* HslV apical surface differs from the *cis* HslV in electrostatic potential (B and C on an identical scale), surface curvature, and pore size.

that domain I unfolds proteins by alternatively exposing and burying its binding site, as described below, rather than through an order–disorder transition [19].

Conformational changes were also previously observed in the central pore of the HslU hexamer [19]. However, the functional role of this pore had not been established, because the pore and nucleotide binding domains of HslU were observed to be remote to HslV in the previous crystal structure [19]. In the current structures, it is clear that this is a translocation pore where the unfolded polypeptide is likely threaded through and translocated into HslV.

The translocation pore consists of a primary and a secondary motif (Figure 2a). The primary motif (pore 1 in Figure 2) forms the innermost pore in the HslU hexamer. This motif contains a conserved GYVG sequence, and is located in sequence next to the Walker box A or P loop motif that binds the phosphate of the nucleotide. The secondary motif (pore 2 in Figure 2) forms a second layer next to the primary pore in the HslU hexamer. This motif is located in sequence immediately next to Walker box B. Nucleotide binding induces conformational changes in Walker box A (and through it to pore 1) as well as in Walker box B (and through it to pore 2). Pore 2 is linked to pore 1 through backbone interactions. Therefore, nucleotide binding induces conformational changes in the pore through two separate paths: directly through Walker A, and indirectly through Walker B and pore 2.

The primary pore motif is conserved among all protease-associated ATPases and the chaperones ClpB and Hsp104 (Figure 2b), implying a shared mechanism. There are only small variations in the second to fourth residues among different subfamilies: the second position is always either Y or F; the third position is hydrophobic; and the fourth position is always G. The consensus sequence at the first position differs among subfamilies. It is G in ClpA, ClpB, ClpC, ClpX, and HslU, it is T in Lon, it is M in FtsH, and it is K in the 19S ATPases. All these ATPases belong to the AAA/AAA+ family, and ClpA, ClpB, ClpC, ClpX, and HslU also belong to the Clp/ATPase family [21–23].

The Bound dADP in HslU Is in an *anti* Conformation

In the structure of the asymmetric HslVU complex, an electron density map unambiguously reveals that the bound dADP is in an *anti* conformation (Figure 1a), rather than in the previously described *syn* conformation [19]. In this *anti* conformation, dADP adenine N1 accepts a hydrogen from Ile-18 amide and N6 donates its hydrogen to Ile-18 carbonyl for two discriminative hydrogen

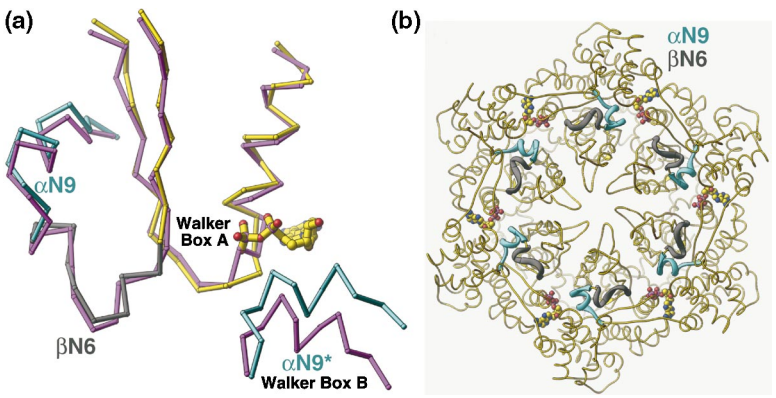

Figure 4. Nucleotide-Dependent Conformational Changes at the Binding Pocket

(a) A superposition of the nucleotide-free HslU subunit (magenta) onto dADP-bound HslU (yellow, gray, and cyan) using Walker box A Cα coordinates reveals conformational changes in Walker box B or helix αN9 (cyan), especially from an adjacent subunit (asterisk).

(b) Helix αN9 (cyan) and strand βN6 (gray) cross-link all 6 HslU subunits with the bound dADP.

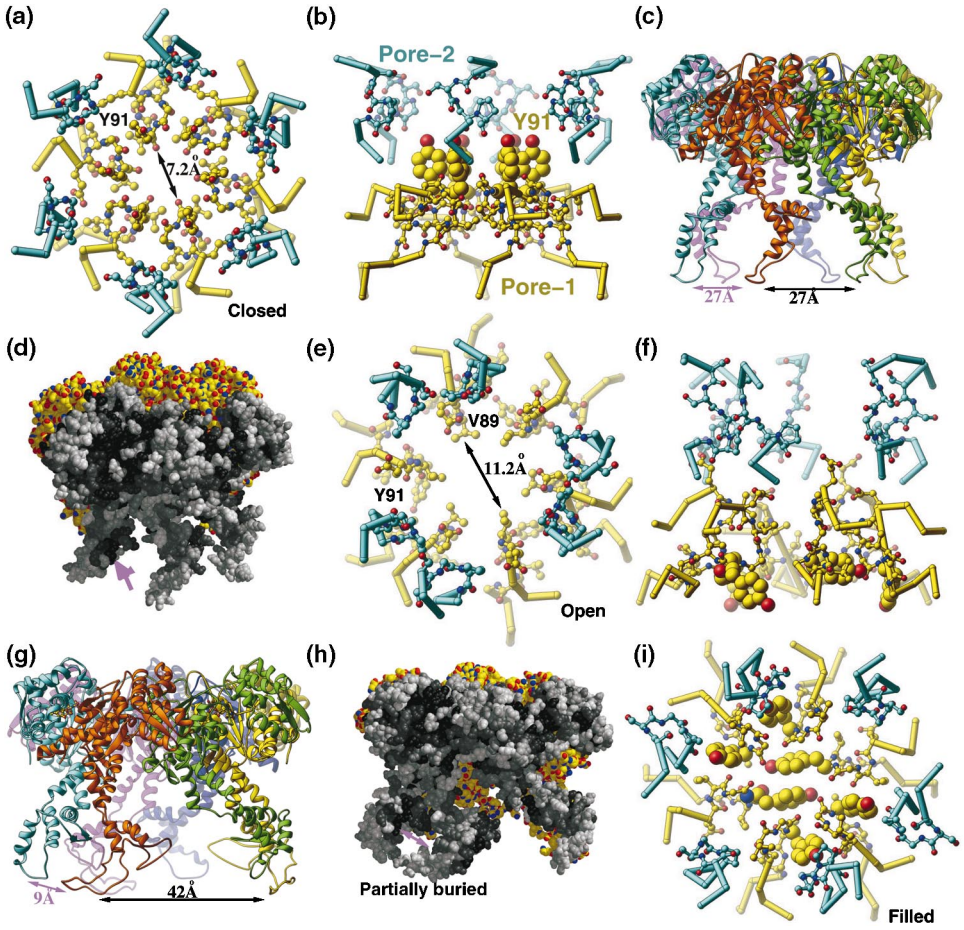

Figure 5. Three HslU Conformational States

Closed (a–d), open (e–h), and filled (i).

(a) The closed state occurs in the dADP-bound HslU structure and a previous structure with 6 AMPPNP bound per HslU hexamer. Pore 1 (yellow) and pore 2 (cyan) are shown. The accessible pore diameter is 4.4 Å (the closest distance between the centers of atoms across the pore is 7.2 Å).

(b) Side view of the closed pore structure.

(c) Domain I in the HslU hexamer is symmetrically distributed in the closed state in the asymmetric complex, in which the missing domain I residues were modeled according to Bochtler et al., [19].

(d) Domain I exposes a substrate binding site in the closed state.

(e) The open state occurs in a previously determined structure with 3 AMPPNP bound per HslU hexamer.

(f) Side view of the open pore structure.

(g) Domain I is asymmetrically distributed in the open state.

(h) A part of conserved surface in domain I is buried between two adjacent HslU subunits.

(i) The filled state occurs in a previously determined structure with 4 ATP bound per HslU hexamer.

bonds (Figure 1a). This recognition pattern explains why HslU is specifically an ATPase [8].

Nucleotide-Dependent Conformational Changes in HslU

Our structures have 6 dADP bound per HslU hexamer. The hexameric HslU assembly in the 3.0 Å asymmetric complex is in essentially the same conformation as the structure of HslU with 6 bound AMPPNP per hexamer [19]. The Cα rms difference was 0.8 Å between the two hexamers. Two structures of the HslU ATPase have also been determined with fewer nucleotides bound, one with 3 AMPPNP and the other with 4 ATP bound per hexamer [19]. Large conformational differences between these various structures are observed and are presumably due to differences in the number and type of the bound nucleotide in them.

We examined the Walker box A and B motifs in HslU in order to determine how conformational changes are transmitted from the nucleotide binding pockets to the rest of the structure. Walker box B consists of residues 318–328 near helix αN9 [18]. We superimposed the nucleotide-free HslU subunit [19] onto the dADP-bound HslU structure using Walker box A Cα coordinates. As a result of this superposition, the Cα coordinates in the Walker box B motif from its neighboring subunit were displaced by up to 7.1 Å with an average displacement of 4.5 Å (Figure 4a). Conformational changes also exist in Walker box B within each HslU subunit, but are relatively small (Figure 4a). It is interesting to note that when the

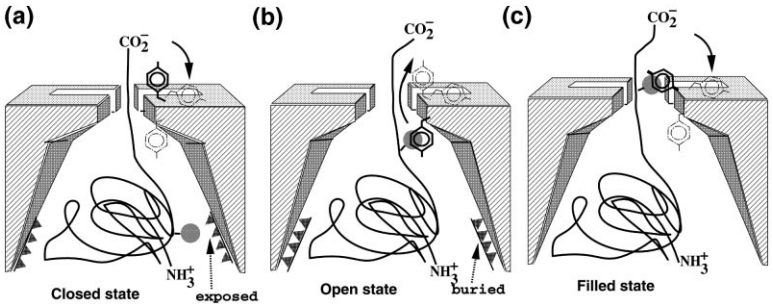

Figure 6. A Protein Unfolding–Coupled Translocation Mechanism

Solid arrows indicate the movement of Y91. Dashed arrows indicate where hydrophobic surface is exposed and buried. Dotted outlines of a tyrosine show positions of Y91 in alternative states. Shaded spheres represent hydrophobic residues from unfolded substrate.

(a) In the closed state, the pore is closed and hydrophilic, and domain I has exposed substrate binding sites for the unfolded protein.

(b) In the open state, the pore is hydrophobic and open, and domain I has partially buried its substrate binding sites. The unfolded protein is released from domain I and may rebind at the pore.

(c) During the open to closed transition, Y91 moves from inside HslU to HslV. If a hydrophobic residue from the unfolded substrate moves with Y91, translocation occurs. As indicated in this figure, small side clefts span the pore. Through these clefts another route exists for Y91 to return from the HslU to HslV side of the pore.

dADP-bound HslU structure is superimposed onto the ADP-bound myosin ATPase structure [24] using Walker box A Cα coordinates, Walker box B occupies a region corresponding to "switch I", and strand βN6, which immediately proceeds Walker box B, occupies a "switch II"-like region.

The inter-subunit conformational changes near the nucleotide binding pocket (Figure 4b) cause extensive repacking of the inter-subunit (HslU–HslU) interface within each HslU hexamer. Since domain I extends out from the subunit interface in the HslU hexamer, repacking of this interface is responsible for large motions of domain I.

There are three HslU conformational states that can be observed in the current and previous structures (Figure 5). (1) The closed state (Figures 5a–5d) occurs in our current HslU structure containing 6 dADP per hexamer as well as the previous structure containing 6 AMPPNP [19]. In this state, the pore diameter is 4.4 Å, the pore is hydrophilic, and Tyr-91 of the GYVG motif points toward HslV. (2) The open state (Figures 5e–5h) has been shown to occur in a previously determined HslU structure with 3 AMPPNP per hexamer [19]. In this state, the pore diameter is 8.4 Å, the pore is hydrophobic, and Tyr-91 points inside HslU. (3). Finally, the filled state (Figure 5i) has also been shown to occur in a HslU structure with 4 ATP bound per hexamer [19]. In this state, two of six Tyr-91 residues occupy the pore. These states suggest that Tyr-91 can move from inside HslU toward HslV through the pore. In addition to changes in the pore structure, domain I undergoes a nucleotide-dependent twisting motion [19]. This motion causes the conserved surface on domain I to be exposed in the closed state and partially buried in the open state (Figures 5d and 5h).

A Protein Unfolding–Coupled Translocation Mechanism

On the basis of our earlier work on ClpP and comparisons of it with HslV and the 20S proteasome, we proposed that the protein substrates of these proteases had to be in an extended conformation before they could be threaded through the central pores into proteolytic chambers [14–15]. In the structures described here, the pores of the HslU ATPase and HslV peptidase are aligned. This juxtaposition provides further evidence for the polypeptide-threading proposal. These structures, however, do not address at which terminus the threading begins and how the terminus is recognized.

Once the threading begins, how is the remaining protein unfolded by the ATPases and translocated through the pores? On the basis of the three HslU conformations described above, we propose a protein unfolding–coupled translocation mechanism (Figure 6). Our mechanism involves the alternate exposure and burial of hydrophobic patches, and is thus reminiscent of the two-stroke unfolding mechanism proposed for GroEL [25–27].

The first step in our mechanistic cycle involves the closed state described above (Figure 6a). In this state, we propose that the pore is clamped around polypeptide substrate. In addition, the exposed hydrophobic surface in domain I would favor unfolding of substrate by providing binding sites for protein in nonnative conformation. The open state, by way of contrast, contains less accessible hydrophobic surface area in domain I (Figure 6b). This would favor the release of unfolded polypeptide by this domain. The released polypeptide could potentially refold in solution. However, in this state, the pore is open and hydrophobic, and provides an excellent and alternative binding site for polypeptide. Binding at the pore site would result in a net transfer of polypeptide from domain I to the pore. A key component of the hydrophobic patch at the pore in this state is provided by Y91. In the filled state (Figure 6c), this residue lies within the pore. It is tempting to speculate that its motion might be coupled to that of the unfolded polypeptide. If it were, then translocation of polypeptide from HslU through its pore into HslV would occur in the transition from filled to closed state, and this translocation would be unidirectional from HslU to HslV.

Biological Implications

ATP-dependent proteolysis is essential for cellular function. ATP-dependent proteases appear to have a shared ATP-dependent proteolysis mechanism on the basis of sequence analysis and structural studies. The bacterial HslVU protease has been a model system for mechanistic studies. The present study reveals that the pores of the ATPase and peptidase are aligned in HslVU, as they are in ClpAP and the 26S proteasome in the EM studies

[16–17]. Therefore, our proposal of a polypeptide-threading mechanism through the aligned pores is likely applicable to all ATP-dependent proteases.

Many of the ATPases in ATP-dependent proteases have a dual function—in addition to serving as peptidase activators, they can act as chaperones [23, 27–32]. The residues that made up the translocation pore in all of these ATPases are conserved, suggesting that the proposed polypeptide-threading mechanism is also relevant to their chaperone activities.

Though we used an equal molar ratio of HslU and HslV in our crystallization trials, we have obtained both asymmetric ($U_6V_6V_6$) and symmetric ($U_6V_6V_6U_6$) HslVU complexes. It is possible that the symmetric complex is the biologically relevant form of HslVU. If it were, the two HslU hexamers would have to coordinate their activities so that (1) substrate binding in one would preclude substrate binding in the other and (2) substrate binding in one would open the translocation pore of the other HslU hexamer, allowing proteolytic products to diffuse away. A simpler and therefore more appealing model would have the asymmetric peptidase-ATPase complex as the biologically active form. In this form, unfolded protein substrates could enter the HslV proteolytic chamber through one end, and proteolytic oligopeptide products diffuse out on the other end. The HslU ATPase actively catalyzes substrate entry through the proposed protein unfolding–coupled translocation mechanism, and it also catalyzes proteolytic product leaving by widening the distal HslV translocation pore. In addition, previously published data on size exclusion chromatography of HslVU indicate a dominant form consistent with a $U_6V_6V_6$ configuration (for example, Figure 5a of [33]). The asymmetric binding of one ATPase (ClpX or ClpA) to the peptidase ClpP was previously observed [34], suggesting that the asymmetric complexes may also be the biologically active form in the ATP-dependent protease.

Our protein unfolding–coupled translocation mechanism requires the hydrophobic interactions of Y91 at the pore with the unfolded protein substrates. Thus, a prediction of the mechanism is that the translocation will stall, and proteolysis will abort, when the ATP-dependent proteolysis machinery encounters a long stretch of amino acids devoid of hydrophobic residues. Such stalling, leading to a defined proteolytic product, has been observed in a glycine-rich region of the NF-κB precursor [35] and near the SulA amino terminus in an MBP-SulA fusion substrate [36].

Experimental Procedures

Crystallization and Data Collection

The *E. coli* enzymes of HslU and HslV were coexpressed, then copurified, and finally separated from each other and further individually purified [6]. An equal molar ratio mixture of the two enzymes in the presence of 1 mM dATP and 20 mM $MgCl_2$ was crystallized in two forms in P321 at room temperature using the hanging drop vapor-diffusion method. The nucleotide dATP was hydrolyzed to dADP during the course of crystallization. Crystal form I was grown in drops containing 1 μl 15 mg/ml HslVU in storage buffer (20 mM Tris-HCl [pH 7.8], 5 mM $MgCl_2$, 0.5 mM EDTA, 1 mM DTT, and 10% glycerol) mixed with 1 μl reservoir solution (10% ethylene glycol, 20 mM $MgCl_2$, 2 mM DTT, and 1 mM EDTA). Form II was grown in drops containing 1 μl 27 mg/ml HslVU in the storage buffer without mixing with the reservoir solution (0.1 M MES [pH 6.3]/1.5 M NaAc). Form I crystals were frozen in the presence of 30% ethylene glycol and form II crystals were frozen after crystals were dipped into paratone-N (Hampton Research). All crystals had various degrees of hemihedral twinning with a twinning operation of (-h, -k, l). The twinning fraction rose to 50% with increasing resolution. Low-resolution data were collected from frozen crystals using an R-axis IV imaging-plate system at home radiation sources and X-ray beam BL6A at the Photon Factory in Japan. The 3.0 Å resolution data were collected at the Advanced Light Source (Berkeley) beam line 5.0.2. Data were processed using the HKL suite of programs [37].

Structure Determination and Refinement

The structures were determined by molecular replacement as implemented in CNS [38] in both forms with low twinning fraction data sets. Search models were hexameric HslU and dodecameric HslV of Bochtler et al. [19]. The structures were refined using CNS. For the form I model, noncrystallographic symmetry (NCS) was only implicitly restrained during the MLHL refinement [38] with external phases. The external phases were calculated in two steps: (1) initial phases and figures of merit were generated by composite-omit simulated-annealing from a partially refined model, and (2) these phases were improved using density modification and 2-fold NCS averaging with an external mask. The mask covered only the model of one twinning fraction. The second twinning portion was suppressed using these external phases and ignored during the refinement. Cyclic detwinning using atomic models was attempted and so was the refinement with the inclusion of a twinning fraction. They did not yield better electron density maps and free R factor values. A part of domain I was partially disordered in the final electron density maps in form I, and it could not be built with certainty (Table 1). Weak electron density was observed near the peptidase active sites. This density could correspond to copurified oligopeptide products or substrates, but no peptides were built into the model. The model for form II was refined only by rigid-body refinement with one body per subunit and fixed $B = 60$ Å^2 for all atoms.

Sequence Alignment

All sequence alignment was carried out using the GCG suite of program (Genetics Computer Group, Inc, Madison, Wisconsin). All sequences of HslU, ClpX, ClpA, ClpC, Lon, FtsH, ClpB, and the proteasome 19S regulator ATPases that were available at the time this work was carried out (March 15, 2000) were included in the alignment. All sequences are from the publicly accessible Swiss-Pro database through PubMed. Individual sequence references are omitted and can be found through PubMed. There were 11 sequences for HslU, 39 for ClpA, ClpB, ClpC, and ClpX, 35 for Lon, and 16 for FtsH at the time.

Figures 1, 4, 5, and 3a were made using the program Ribbons [39], and Figures 3b and 3c were made using the program GRASP [40].

Acknowledgments

J. W. thanks T. A. Steitz (NIH GM-22778) for financial support. This work was in part supported by the Brain Korea 21 project, and the grants of the Korea Science and Engineering Foundation (C. H. C) and the Korea Ministry of Science and Technology (Critical Technology 21 to S. H. E). We are grateful to Drs. N. Sakabe and S.W. Suh for the data collection at Photon Factory (BL6A), Japan.

Received: November 7, 2000
Revised: January 8, 2001
Accepted: January 9, 2001

References

1. Maurizi, M.R. (1992). Proteases and protein degradation in Escherichia coli. Experientia *48*, 178–201.
2. Gottesman, S. (1996). Proteases and their targets in Escherichia coli. Annu. Rev. Genet. *30*, 465–506.
3. Goldberg, A.L. (1992). The mechanism and functions of ATP-dependent proteases in bacterial and animal cells. Euro. J. Biochem *203*, 9–23.

4. Chung, C.H. (1993). Proteases in Escherichia coli. Science *262*, 372–374.
5. Chung, C.H., Yoo, S.J., Seol, J.H., and Kang, M.S. (1997). Characterization of energy-dependent proteases in Escherichia coli. Biochem. Biophys. Res. Commun. *24*, 613–616.
6. Yoo, S.J., and Chung, C.H. (1996). Purification and characterization of the heat shock proteins HslV and HslU that form a new ATP-dependent protease in Escherichia coli. J. Biol. Chem. *271*, 14035–14040.
7. Missiakas, D., Schwager, F., Betton, J.M., Geogopoulos, C., and Raina, S. (1996). Identification and characterization of HslV HslU (ClpQ ClpY) proteins involved in overall proteolysis of misfolded proteins in Escherichia coli. EMBO J. *15*, 6899–6909.
8. Rohrwild, M., and Goldberg, A.L. (1996). HslV-HslU: A novel ATP-dependent protease complex in Escherichia coli related to the eukaryotic proteasome. Proc. Natl. Acad. Sci. USA *93*, 5808–5813.
9. Kessel, M., Wu, W., Gottesman, S., Kocsis, E., Steven, A.C., and Maurizi, M.R. (1996). Six-fold rotational symmetry of ClpQ, the E. coli homology of the 20S proteasome, and its ATP-dependent activator, ClpY. FEBS Lett. *398*, 274–278.
10. Chuang, S.E., Burland, V., Plunkett, G., 3rd, Daniels, D.L., and Blattner, F.R. (1993). Sequence analysis of four new heat-shock genes constituting the hslTS.ibpAB and hslVU operons in Escherichia coli. Gene *134*, 1–6.
11. Lowe, J., Stock, D., Jap, B., Zwickl, P., Baumeister, W., and Huber, R. (1995). Crystal structure of the 20S proteasome from the archaeon T. acidophilum at 3.4Å resolution. Science *268*, 533–539.
12. Groll, M., and Huber, R. (1997). Structure of 20S proteasome from yeast at 2.4Å resolution. Nature *386*, 463–471.
13. Bochtler, M., Ditzel, L., Groll, M., and Huber, R. (1997). Crystal structure of heat shock locus (HslV) from Escherichia coli. Proc. Natl. Acad. Sci. USA *94*, 6070–6074.
14. Wang, J., Hartling, J.A., and Flanagan, J.M. (1997). The structure of ClpP at 2.3Å resolution suggests a model for ATP-dependent proteolysis. Cell *91*, 447–456.
15. Wang, J., Hartling, J.A., and Flanagan, J.M. (1998). Crystal structure determination of Escherichia coli ClpP starting from an EM-derived mask. J. Struct. Biol *124*, 151–163.
16. Beuron, F., and Steven, A.C. (1998). At sixes and sevens: characterization of the symmetry mismatch of the ClpAP chaperone-assisted protease. J. Struct. Biol *123*, 248–259.
17. Zwickl, P., Baumeister, W., and Steven, A. (2000). Dis-assembly lines: the proteasome and related ATPase-assisted proteases. Curr. Opin. Struct. Biol. *10*, 242–250.
18. Rohrwild, M., and Goldberg, A.L. (1997). The ATP-dependent HslVU protease from Escherichia coli is a four-ring structure resembling the proteasome. Nature Struct. Biol *4*, 133–139.
19. Bochtler, M., Hartmann, C., Song, H.K., Bourenkov, G.P., Bartunik, H.D., and Huber, R. (2000). The structures of HslU and the ATP-dependent protease HslU-HslV. Nature *403*, 800–805.
20. Richards, F.M. (1985). Calculation of molecular volumes and areas for structures of known geometry. Methods Enzymol. *115*, 440–464.
21. Neuwald, A.F., Aravind, L., Spouge, J.L., and Koonin, E.V. (1999). AAA+: a class of chaperone-like ATPases associated with the assembly, operation, and disassembly of protein complexes. Genome Res *9*, 27–43.
22. Zwickl, P., and Baumeister, W. (1999). AAA-ATPases at the crossroads of protein life and death. Nature Cell. Biol *1*, E97–98.
23. Schirmer, E.C., Glover, J.R., Singer, M.A., and Lindquist, S. (1996). HSP100/Clp proteins: a common mechanism explains diverse functions. Trends Biochem. Sci. *21*, 289–296.
24. Smith, C.A., and Rayment, I. (1996). Active site comparisons highlight structural similarities between myosin and other P-loop proteins. Biophys. J. *70*, 1590–1602.
25. Xu, Z., Horwich, A.L., and Sigler, P.B. (1997). The crystal structure of the asymmetric GroEL-GroES-(ADP)7 chaperonin complex. Nature *388*, 741–750.
26. Xu, Z., and Sigler, P.B. (1998). GroEL/GroES: structure and function of a two-stroke folding machine. J. Struct. Biol *124*, 129–141.
27. Seong, I.S., Oh, J.Y., Lee, J.W., Tanaka, K., and Chung, C.H. (2000). The HslU ATPase acts as a molecular chaperone in prevention of aggregation of SulA, an inhibitor of cell division in Escherichia coli. FEBS Lett. *477*, 224–229.
28. Horwich, A.L., Weber-Ban, E.U., and Finley, D. (1999). Chaperone rings in protein folding aand degradation. Proc. Natl. Acad. Sci. USA *96*, 11033–11040.
29. Weber-Ban, E.U., Reid, B.G., Miranker, A.D., and Horwich, A.L. (1999). Global unfolding of a substrate protein by the Hsp100 chaperone ClpA. Nature *401*, 90–93.
30. Wickner, S., Maurizi, M.R., and Gottesman, S. (1999). Posttranslational quality control: folding, refolding, and degrading proteins. Science *286*, 1888–1893.
31. Levchenko, I., Luo, L., and Baker, T.A. (1995). Dissembly of the Mu transposase by the ClpX chaperone. Genes Dev. *9*, 2399–2408.
32. Benaroudj, N., and Goldberg, A.L. (2000). PAN, the proteasome-activating nucleotidase from archaebacterium, is a protein-unfolding molecular chaperone. Nature Cell Biol. *2*, 833–839.
33. Yoo, S.J., Seol, J.H., Seong, I.S., Kang, M.S., and Chung, C.H. (1997). ATP binding, but not its hydrolysis, is required for assembly and proteolytic activity of the HslVU protease in Escherichia coli. Biochem. Biophys. Res. Comm *238*, 581–585.
34. Girmaud, R., Kessel, M., Beuron, F., Steven, A.C., and Maurizi, M.R. (1998). Enzymatic and structural similarities between the Escherichia coli ATP-dependent proteases, ClpXP and ClpAP. J. Biol. Chem. *273*, 12476–12481.
35. Lin, L., and Ghosh, S. (1996). A glycine-rich region in NF-κB p105 functions a processing signal for the generation of p50 subunit. Mol. Cell. Biol. *16*, 2248–2254.
36. Seong, I.S., Oh, H.Y., Yoo, S.J., Seol, J.H., and Chung, C.H. (1999). ATP-dependent degradation of SulA, a cell division inhibitor, by the HslVU protein in Escherichia coli. FEBS Lett. *456*, 211–214.
37. Otwinowski, Z., and Minor, W. (1997). Processing of x-ray diffraction data collected in oscillation mode. Methods Enzymol. *276*, 307–325.
38. Brunger, A.T., and Warren, G.L. (1998). Crystallography & NMR system: a new software suite for macromolecular structure determination. Acta Crystallogr. *D50*, 905–921.
39. Carson, M. (1991). Ribbons 2.0. J. Appl. Cryst. *24*, 958–961.
40. Nicholls, A., Sharp, K.A., and Honig, B. (1991). Protein folding and association: insights from the interfacial and thermodynamic properties of hydrocarbons. Proteins Struct. Funct. Genet. *11*, 282–296.
41. Sousa, M.C., Trame, C.B., Tsuruta, S., Wilbanks, S.M., Reddy, V.S., and McKay, D. (2000). Crystal and solution structures of an HslUV protease-chaperone complex. Cell *103*, 633–643.
42. Ishikawa, T., Maurizi, M.R., Belnap, D., and Steven, A.C. (2000). Docking of components in a bacterial complex. Nature *408*, 667–668.
43. Bochtler, M., Hartmann, C., Song, H.K., Bourenkov, G.P., Bartunik, H.D., and Huber, R. (2000). Docking of components in a bacterial complex. Nature *408*, 668.
44. Song, H.K., and Huber, R. (2000). Mutational studies of HslU and its docking mode with HslV. Proc. Natl. Acad. Sci. USA *97*, 14103–14108.
45. Ortega, J., Singh, S.K., Ishikawa, T., Maurizi, M.R., and Steven, A.C. (2000). Visualization of substrate binding and translocation by the ATP-dependent protease, ClpXP. Mol. Cell *6*, 1515–1521.

Note Added in Proof

While this manuscript was under review, four publications [41–44] on HslVU structures and one [45] on the translocation mechanism of an ATP-dependent protease appeared in print. One crystal structure, small-angle X-ray scattering data, and an additional EM structure [41–42] agree with our crystal structures of the HslVU complex. An EM structure of another ATP-dependent protease is also consistent with our mechanism [45]. Huber and colleagues have presented another HslVU complex [44]. However, there were no systematic extinctions along (00*l*) with $l = 2n + 1$ in the observed data, which argued against their space group assignment of $P6_322$ for the complex.